SAND2019-3880C

Robust Lidar Data Processing and Quality Control Methods Developed for the SWiFT Wake Steering Experiment

T G Herges[1], and P Keyantuo[1]

[1]Sandia National Laboratories, Albuquerque, NM, 87185, United States of America

Abstract. Sandia National Laboratories and the National Renewable Energy Laboratory conducted a wake-steering field experiment at the Scaled Wind Farm Technology facility. The campaign included the use of two highly instrumented V27 wind turbines, an upstream meteorological tower, and high-resolution wake measurements of the upstream wind turbine using a customized scanning SpinnerLidar from the Technical University of Denmark. The present work details how the SpinnerLidar data uploaded to the Department of Energy Atmosphere to Electrons Data Archive and Portal was processed, quality controlled and assured to guarantee high data availability with the removal of invalid measurements. A multi-dimensional approach to processing the SpinnerLidar Doppler spectra was developed based on matching erroneous measurements within the two-dimensional lidar scan with patterns inside the multidimensional lidar Doppler spectra. This method allows image processing techniques to be used to remove regions of the Doppler spectra that are contaminated by hard targets and isolate the velocity field of interest, allowing more accurate line-of-sight velocity measurements and enabling the estimation of the turbulence of the line-of-sight velocities within the probe volume.

1. Introduction

Wind turbine wake structure, evolution, and dynamics are produced by a complex interaction of the atmospheric conditions and wind turbine characteristics [1]. Understanding and predicting these interactions with credibility can be challenging for many modelling tools [2]. Thus, straightforward data of sufficient quality for validation with simple boundary conditions are needed to help understand these interactions and improve model development with increased confidence [3]. An important aspect for producing data of appropriate quality for conducting validation is ensuring that the data have been accurately quality controlled and assured prior to use. The quality assurance and control (QA/QC) methods confirm the quality of data and that erroneous measurements, which could misinform future analyses, are removed.

A team of researchers at Sandia National Laboratories (SNL) conducted a field experiment at the Department of Energy (DOE)/SNL Scaled Wind Farm Technology (SWiFT) facility [4] to investigate wind turbine yaw control on the performance of an aligned pair of wind turbines and produce validation data by measuring the inflow, turbine response, and wake characteristics. The field test measured the power and loads of the upstream turbine under various yaw offset angles in addition to the power and loads of the downstream turbine versus the upstream wake position [5]. The experiment included the use of the Technical University of Denmark (DTU) SpinnerLidar, which was uniquely capable of measuring the wake at the temporal and spatial resolution required for the experiment, to characterize the wake dynamics and velocity deficit measurements under various inflow conditions and upstream wind turbine yaw offsets [1, 5-7]. Data collected as part of the multi-month field campaign have been made publicly available through the DOE Atmosphere to electron (A2e) Data Archive and Portal (DAP) to support model development and further verification and validation efforts by the international research community [8].

The present work details the QA/QC methodology and process developed to ensure the quality of the DTU SpinnerLidar data by filtering out invalid measurements and maximizing data availability within the completed lidar scans, treated as a two-dimensional cross-plane of data. Many common filtering techniques such as despiking, deholding, thresholding, and derivative-based methods have been developed for filtering out invalid measurements with traditional meteorological tower and wind turbine response data [4, 9], but a universal approach that is applicable for all scenarios of lidar measurement remains incomplete. Scanning lidars create a greater challenge for a universal QA/QC method, valid in all flow scenarios, since the probe location moves in multiple dimensions throughout the fluctuating flowfield. Traditionally, the signal-to-noise ratio (SNR) of the returned lidar signal has been used to assess quality of the measurement [10, 11]. Adaptive SNR or carrier-to-noise ratio (CNR) filtering techniques have been implemented successfully for lidar data QA/QC [12] in addition to finite difference despiking methods [13]. However, these methods do not address many of the data quality issues.

The current work uses a combination of techniques to ensure the quality of the SpinnerLidar data. The techniques were developed based on matching erroneous measurements within the lidar scan rosette to patterns, or features, within the multidimensional lidar Doppler spectra. The QA/QC approach uses feature identification of hard targets, low-signal return, and returns from operational wind turbine blades within the Doppler spectra to remove those measurements. A two-dimensional neighborhood filter with time weighting catches any additional invalid measurements. This outlier detection was developed as a two-dimensional implementation of traditional despiking methods. These new QA/QC and Doppler spectra processing methods allow for more accurate line-of-sight velocity measurements in addition to enabling the estimation of the turbulence of the line-of-sight velocity within the lidar probe volume.

2. Experimental Setup

Sandia National Laboratories operates the SWiFT facility located in Lubbock, Texas. The baseline site instrumentation includes three research wind turbines (WTG) and two meteorological towers (MET) as shown in figure 1a.

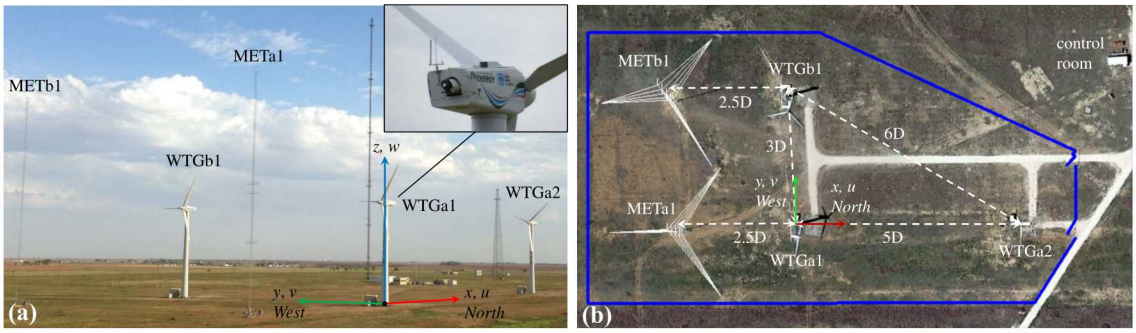

Figure 1. (a) SWiFT site layout and coordinate system with the DTU SpinnerLidar installed in WTGa1 (b) including a top view of the facility layout [14], where D = 27 m.

The layout of the SWiFT facility is seen from an overhead view in figure 1b. The meteorological tower and the two turbines used in this campaign (METa1, WTGa1, and WTGa2) are all aligned with the predominant wind direction at the site, 180 degrees (north is 0 degrees). This configuration allows measurement of the atmospheric inflow with the meteorological tower and measurement of the wake of the WTGa1 turbine using the nacelle-mounted DTU SpinnerLidar. The SWiFT turbines are highly-modified, variable speed, collective pitch Vestas V27 machines with a hub height of 32.1 meters, a rotor diameter of 27 m, and a maximum power output of 192 kW [14].

DTU developed the SpinnerLidar to be a turbine mounted lidar for rapid scanning of the wind field in a two-dimensional plane. The SpinnerLidar was uniquely capable of measuring the wake of WTGa1 at the temporal and spatial resolution required for this experimental campaign. For this experiment, the SpinnerLidar was mounted as shown in figure 2 to point out of the rear of the upwind (WTGa1) turbine nacelle, optimally positioned to capture the full wind turbine wake between one and five rotor diameters

downstream (D = 27 m). The SpinnerLidar has a scan head consisting of two co-rotating ~15° wedge-shaped prisms integrated on a ZephIR 300 continuous-wave coherent Doppler lidar. The lidar produces laser light at a wavelength of 1565 nm and was configured to stream averaged-Doppler spectra at a rate of about 492 measurements per second. The prisms have a fixed gear ratio with adjustable motor settings to change the duration and number of measurements per scan (motor speed was fixed for each scan) [15, 16]. The resulting rosette scan pattern is displayed in figure 2. The SpinnerLidar scans the two-dimensional surface of a sphere with an approximately 30° half angle in the fixed rosette pattern, acquiring 984 line-of-sight velocity measurements in 2 seconds [1]. The lidar can also cycle through focus distances, changing focus distance in the same amount of time as a full scan. The position of the measurement relative to the symmetry axis is calculated from the instantaneous position of the two wedge-shaped prisms. Changes in the orientation of the rotation axis are accounted for using an integrated three-axis accelerometer.

The lidar scan configuration changed throughout the field campaign to both capture wake evolution over multiple focus distances (every ≈ 30 to 42 s with 5 to 7 focus distances, respectively) and wake dynamics concentrating at one focus distance (every ≈ 2 s). The SpinnerLidar was either angled at – 0.4° or – 15.1° relative to the nacelle to capture the wake at different wind turbine yaw offsets (between – 18° to 25°) throughout the course of the experiment.

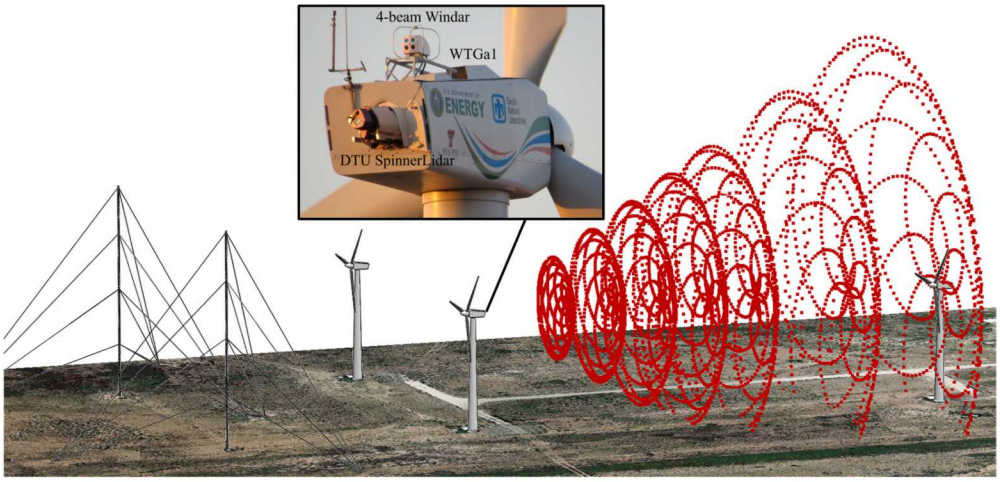

Figure 2. Schematic of the SWiFT facility including the DTU SpinnerLidar scan patterns at seven downstream focus distances from one to five rotor diameters and an image of the installed DTU SpinnerLidar in the rear of WTGa1.

The location of the measurements in the lidar coordinate system were scaled from an initial normalized frame using the average focus distance over the scan (see Ref. [1]). The orientation and position of the lidar relative to the ground and nacelle was determined using total station theodolite (TST) measurements [17]. The lidar roll and pitch angles were measured by a calibrated 3-axis accelerometer [17], and applied to the data to create the lidar coordinate system. The lidar coordinate system is transformed into other coordinate systems as described in Ref. [1].

3. Results

A multi-dimensional approach to processing the SpinnerLidar Doppler spectra was developed to adequately filter out invalid measurements and maximize data availability. This approach allows common image processing techniques to be used to remove regions of the Doppler spectra that are contaminated with invalid measurements. A single 2-second example scan with 984 points, or scan indexes, was chosen to demonstrate the SpinnerLidar QA/QC methods clearly, but these methods were developed and hold for all DTU SpinnerLidar data collected at the SWiFT site, including data with inflow variations in wind speed, turbulence, shear, veer, and aerosol particulate concentrations

throughout all focus distances and motor speed rates. This example scan includes all the primary conditions when invalid measurements occur, including stationary hard target returns from the ground, boresight, downstream turbine with a non-stationary rotor, and low-signal return. This section presents the QA/QC methodology as applied to this scan, going from the raw lidar retrievals (figure 3) to the final line-of sight velocities (figure 10).

The unprocessed SpinnerLidar Doppler spectra acquired during the single example scan are displayed in figure 3a. Figure 3a shows the normalized probability density function (PDF) of velocities, from 0 to 38.25 m/s, within the probe volume of the lidar at each of the 984 scan locations or indexes. The SpinnerLidar produces velocity measurements at 984 scan indexes as shown in figure 3b. The line-of-sight velocity was calculated from the median value of frequencies in the normalized Doppler spectra PDF. Figure 3c shows seven example Doppler spectral traces from which the median frequencies were calculated, while figure 3a is the resulting image from all 984 spectral traces with a distribution of 256 velocity bins from 0 to 38.25 m/s. In this scan, the line-of-sight velocity (v_{los}) was measured at 5D (135 m) downstream while the downstream turbine (WTGa2) was operating.

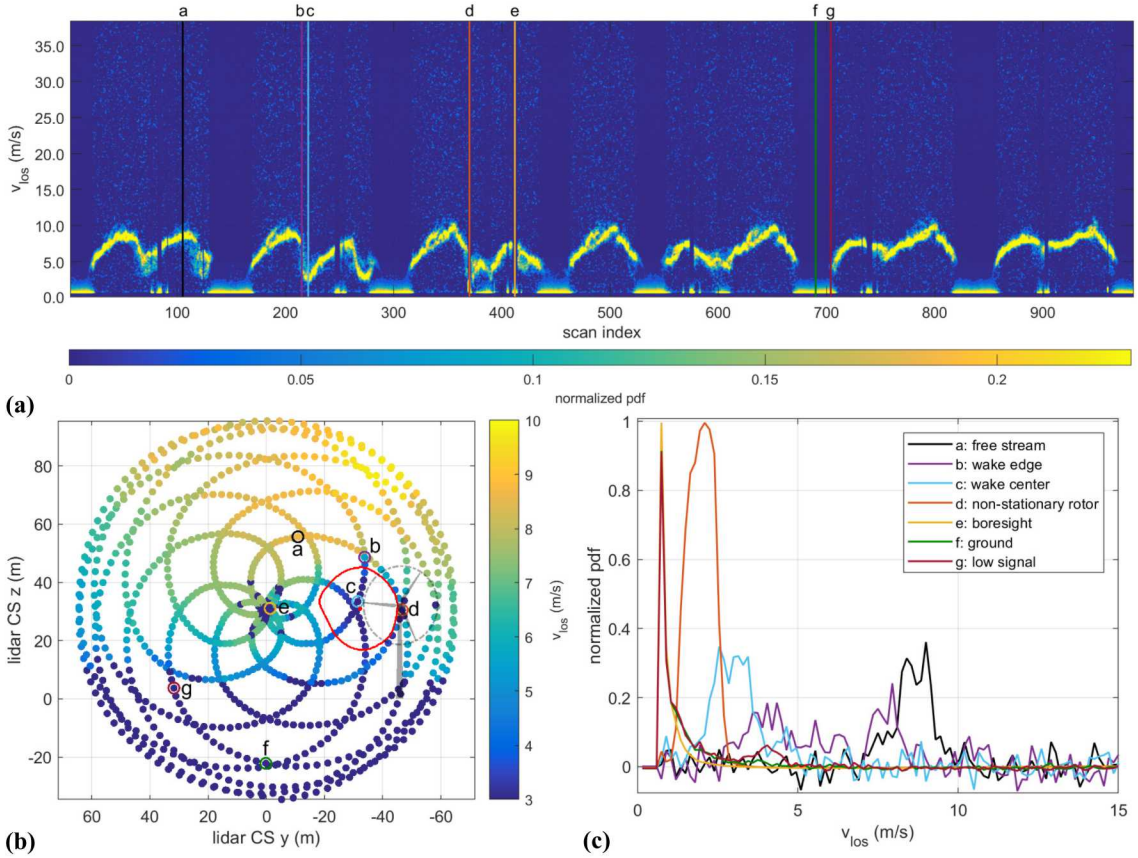

Figure 3. Unprocessed Doppler spectra (a) image with lines indicating the example Doppler distributions, (b) scan pattern with wake (red line and center dot), downstream turbine outlined, and example cases marked with circles and labelled, and (c) normalized PDF's of Doppler power spectra traces for each of the circles in (b) and lines in (a). In part (b), y and z are the lateral and vertical coordinates, respectively.

Seven spectral traces of interest were chosen to help demonstrate the effects of the QA/QC process on this single lidar scan, shown in figures 3 – 10. The velocity distributions of interest include an example of the undisturbed free stream of the atmospheric boundary layer, the center of the wake, the edge of the wake, a boresight return, a ground return, and a return from the rotating downstream rotor.

Figure 3c displays the example Doppler traces, or velocity distributions, with lines and labels of corresponding color indicating where they occur in the Doppler spectral image (figure 3a) and physical scan locations (figure 3b). The free stream, wake center, and wake edge example velocity distributions will remain relatively unchanged while the invalid measurements from the boresight, ground, and nonstationary rotor returns are removed. The boresight returns are due to laser reflections from the outer window of the SpinnerLidar and appear at the center of the scan pattern. Figure 3b shows the corresponding v_{los} with invalid measurements at the center of the scan pattern from the boresight reflections, in addition to the low speed regions near the ground and WTGa2. An outline of WTGa2 and the wake from WTGa1, tracked using the fully quality-processed data and marked by a red outline and center point, are included in figure 3b for reference of what was physically occurring at the locations in the scan relative to the seven example locations.

The spectral image that includes all 984 velocity distributions in figure 3a also provides patterns for indicating the hard target returns from stationary objects. Note the six boresight reflections near 0 m/s in figure 3a near scan indexes 84, 248, 412, 576, 740, and 904, and the ground returns near scan indexes 0, 150, 298, 384, 450, 538, 604, 690, 838, and 984. The boresight and ground returns appear to influence the Doppler spectra between approximately 0 to 2.5 m/s. Vibrations and movement of the SpinnerLidar while the turbine was operating causes the signal from stationary objects to contaminate nonzero velocity bins due to the distortion of the large signal returns from hard targets relative to the backscatter from aerosol particulates. This result effectively measures the displacement motion of the lidar. Theoretically the lidar is capable of measuring velocities as low as 0.15 m/s when not experiencing vibration or motion, but while operating in the nacelle at the SWiFT site, the lidar could measure as low as approximately 2.5 m/s. The influence of the stationary hard target returns is clear in the boresight, ground, and low signal Doppler spectral PDF's (figure 3c). The low signal return case has a strong normalized ground return (≈ 1) in addition to a weak normalized return (≈ 0.06) from the aerosols in the velocity field. This case includes returns from both the ground and atmospheric aerosols due to the large probe volume weighting on the lidar measurements at a focus distance of 5D, where the full width at half maximum is 32.90 m.

Also observe the shot noise in the Doppler spectra image as speckles in figure 3a and noise in the Doppler spectra PDFs in the free stream, wake center, and wake edge distributions in figure 3c due to the fact that many lidar devices are shot noise limited [18]. The shot noise in the Doppler spectra depends inversely on the number of photoelectrons collected by the SpinnerLidar because the shot noise of the signal photons equals the square root of the number of photoelectrons collected. Thus, the shot noise increases with weaker laser signal returns. Each Doppler spectra PDF was acquired over 0.002 s, if the signal was acquired over a longer period the signal return strength would be greater and the noise in the spectra PDFs would be reduced. However, this would increase the time a single scan takes, or reduce the number of measurement points within a scan, reducing the temporal and spatial resolution of the scan. Thus, there is a trade-off between reducing shot noise and acquiring data at the required resolution.

The first step in the QA/QC process of the SpinnerLidar data from the SWiFT facility wake steering experiment was to remove the effect of hard target returns in the Doppler spectral image. Figure 4 shows a mask created from the hard target returns to remove those regions of interest from the spectral normalized PDF image. The mask, or region to remove from the Doppler spectra image, was created by proportionally projecting the signal strength at 0 m/s into higher velocity bins. The values for the linear projection were determined empirically and would vary between lidar devices. However, the values held for the SpinnerLidar throughout all focus distances. The mask regions were then increased horizontally by 2 pixels using the image processing technique of morphological dilation to ensure the regions fully masked the effect of the hard targets in the Doppler spectra. Figure 5a displays the corresponding normalized PDF of the Doppler spectra with the mask region of the boresight and ground returns removed. The resulting ground and boresight examples are removed from the scan (figure 5b) and normalized spectral traces (figure 5c). Also note that the high-strength ground return portion of the low signal example was removed while the low-strength portion, returned from the aerosols, remains. Regions of the scan from both boresight and ground returns remain in the data to be removed with additional QA/QC steps.

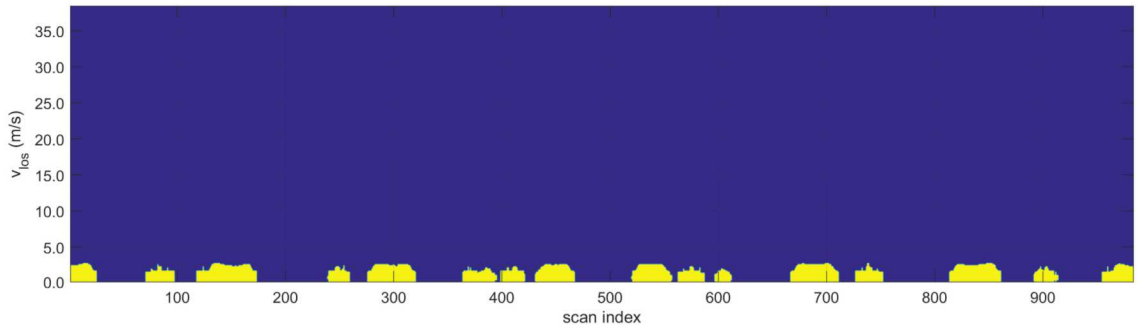

Figure 4. Boresight and ground return mask regions for the Doppler spectra image. The yellow indicates the stationary hard target regions to remove from the Doppler spectra image in figure 3a.

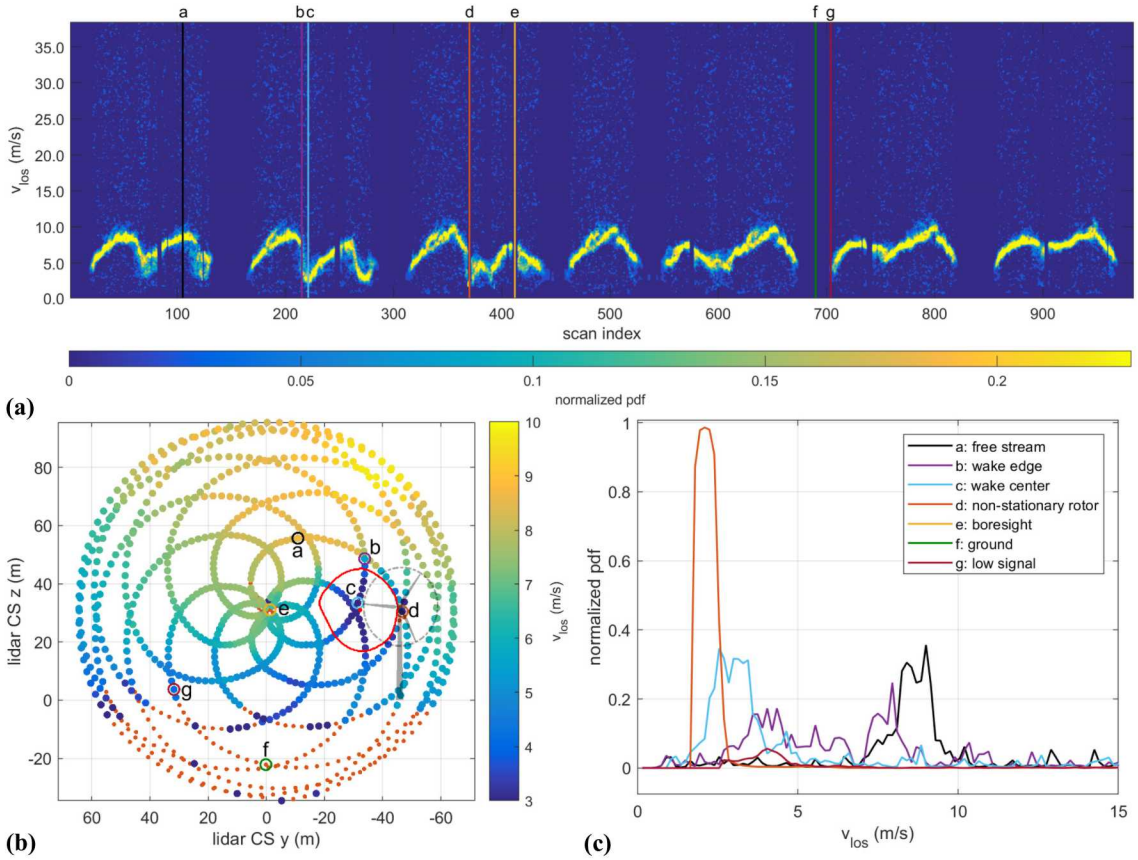

Figure 5. Stationary hard target returns removed, and bilateral shot noise filtered Doppler spectra (a) image with lines indicating the example Doppler distributions, (b) scan pattern with wake (red line and center dot), downstream turbine outlined, and example cases marked with circles and labelled, and (c) example normalized PDF's of Doppler power spectra traces.

A weak bilateral filter was also applied to the Doppler spectra data in figure 5 to reduce the effect of shot noise in the data. The effect can most clearly be seen by comparing the free stream Doppler spectra from figures 3c and 5c in figure 6. Bilateral filters are a common filtering technique for reducing shot noise within images [19]. A bilateral filter is an edge preserving nonlinear filter that replaces the intensity of each pixel with a Gaussian weighted average of intensity values from nearby pixels. The values for the filter were carefully chosen to preserve the normalized Doppler spectral traces throughout

regions with aerosol returns while removing the effects of shot noise. It was believed that a two-dimension noise filter, applied to the Doppler spectra normalized PDF image, would be more effective and accurate at reducing the Doppler spectra noise as compared to a one-dimensional filter that utilizes less information in the filtering process since the flowfield is continuous without discontinuities in the line-of-sight velocity. Comparing the PDF's in figure 6, it appears the bilateral filter adequately preserves the velocity data in the region of interest while reducing the shot noise.

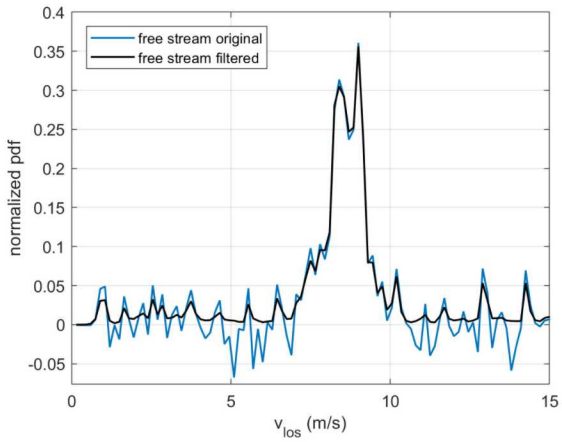

Figure 6. Comparison of free stream normalized PDF's of Doppler power spectra to show the effect of the bilateral filter (figure 5c) as compared to the original PDF (figure 3c).

Next, the effects in the Doppler spectra normalized PDF's away from the velocity regions of interest need to be removed. Therefore, the next step in the QA/QC process was to create a mask for the region of interest in the Doppler spectra using a threshold of any signal above 0.03 (figure 7). This thresholding value was chosen as a value that approaches zero but remains insensitive to the effects of shot noise. Any small regions away from the primary flowfield regions of interest were removed as invalid measurements since the velocity field was continuous and those measurements would either be due to noise or a signal return from a rotating blade.

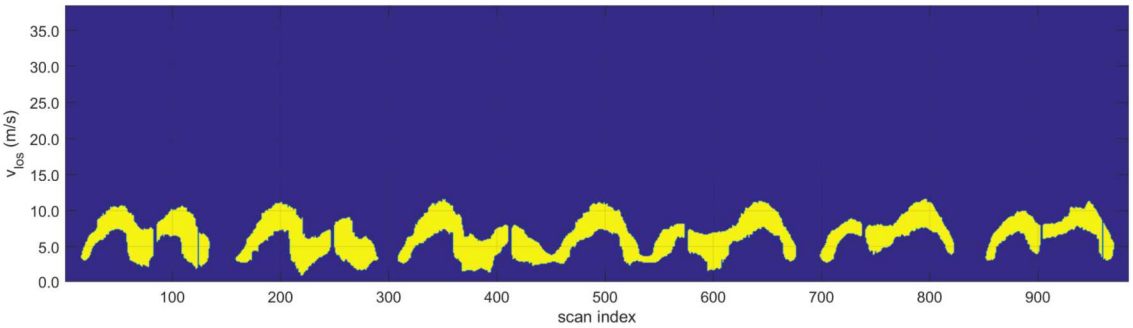

Figure 7. Doppler spectra image regions of interest mask. The yellow regions indicate the regions of interest to keep, zeroing all other regions, in the Doppler spectra image in figure 5a.

Figure 8 presents the Doppler spectra consisting of the regions of interest. The noise has been removed leaving only areas corresponding to the measured velocity field of the atmospheric boundary layer and wake, along with signal returns from the rotating downstream rotor and areas with low SNR. In this case, the invalid returns from the rotating downstream rotor only remain because the downstream turbine was waked and the velocity of the flowfield near the rotor was close to the velocity returned from the rotor as a hard target. Any measurements lower than ground level at the focus distance have

also been removed. The SWiFT facility is very flat resulting in a simple threshold of removing any measurements below $z = 0$ m.

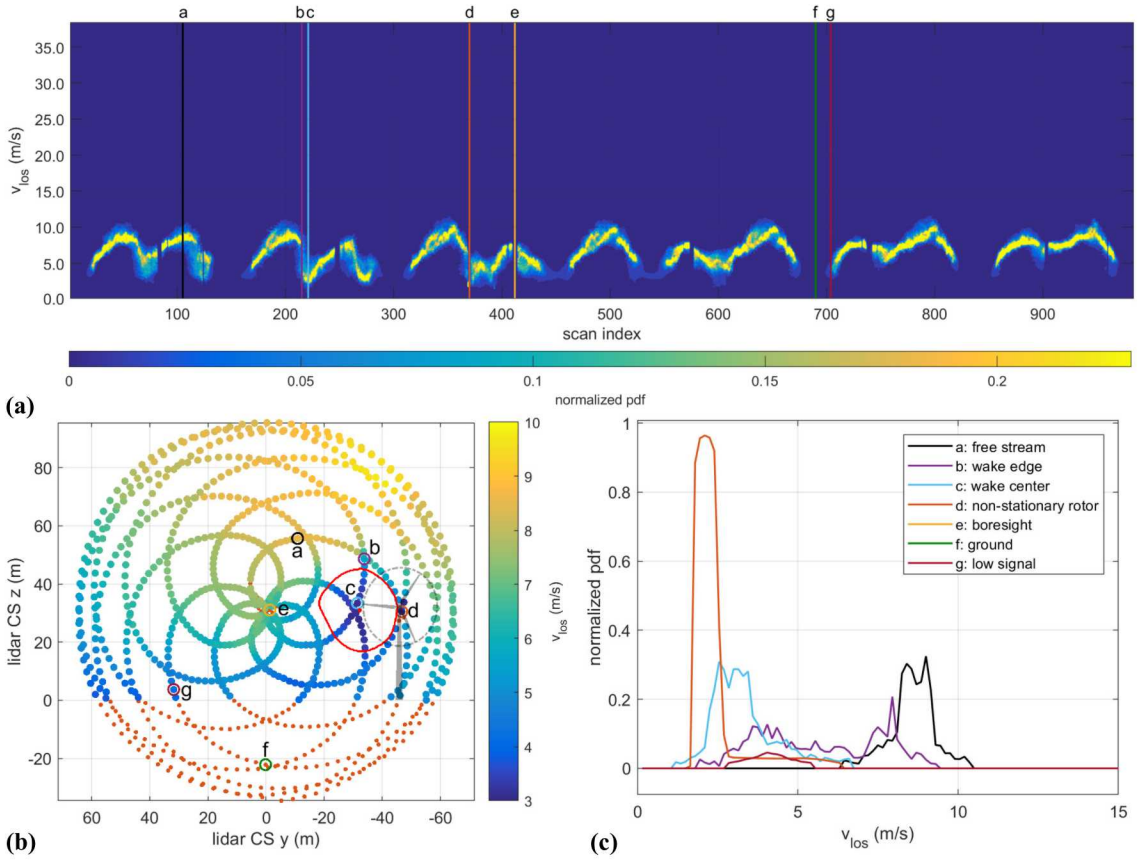

Figure 8. Regions of interest Doppler spectra (a) image with lines indicating the example Doppler distributions, (b) scan pattern with wake (red line and center dot), downstream turbine outlined, and example cases marked with circles, and (c) example normalized PDF's of Doppler power spectra traces.

A more advanced outlier detection method was required to capture returns from the nonstationary hard targets when the flowfield in that region has a similar velocity. Figure 9a shows a spatially smoothed scan pattern using the time-weighted average v_{los} value within a sliding neighbourhood of the black circle. The area of the circle remained constant relative to the scan pattern for all focus distances when this method was applied to other scans. Though the lidar scan pattern has been visualized as a single image or snapshot, the pattern was acquired over time, meaning that the flowfield likely varied during the scan. This velocity variation causes a neighborhood smoothing function to return spikes, or outliers, where the scan pattern crosses, or intersects, with itself because the velocity may be lower, or higher, on the second pass as compared to the first if the velocity field was changing. An example of one of these crossing points in the scan pattern occurs near the wake center in figure 9a. The time-weighting aspect of the neighborhood filter had to be included to give a higher weighted average to velocities acquired closer in time to the measurement point of interest then other velocities within the neighborhood since the velocity field could have varied between scan path crossings. Figure 9b presents the corresponding difference between the spatially-smoothed scan pattern and the unfiltered pattern. The two invalid measurements from the rotating blades are visible in figure 9b and were identified using a threshold of velocity difference ($v_{los} - v_{filter}$) above six standard deviations of the velocity-difference signal.

However, this velocity metric was not robust enough to work for all scenarios of data captured during this field test without including an additional parameter within the outlier detection. Figure 9c shows the peak value of the filtered Doppler spectra PDF at each scan point. Again, the peak return signals from the operational rotor are clear. A threshold of the mean peak value of the Doppler return PDF throughout the 984 scan points plus four standard deviations detected peak signal outliers. The velocity and signal peak outlier detections were combined to robustly capture the effect of the operational rotor at all focus distances, removing only data that qualified as outliers using both detection methods and effectively removing the erroneous non-stationary targets. This methodology held for all scans containing non-stationary returns no matter the focus distance or location of the target relative to the pattern. The number of standard deviations needed for the velocity threshold and peak signal threshold were empirically determined using numerous scans, but the methodology of combining a velocity outlier detection and peak signal return outlier detection could be used for other lidar data sets or lidar devices once the standard deviation bounds were assessed.

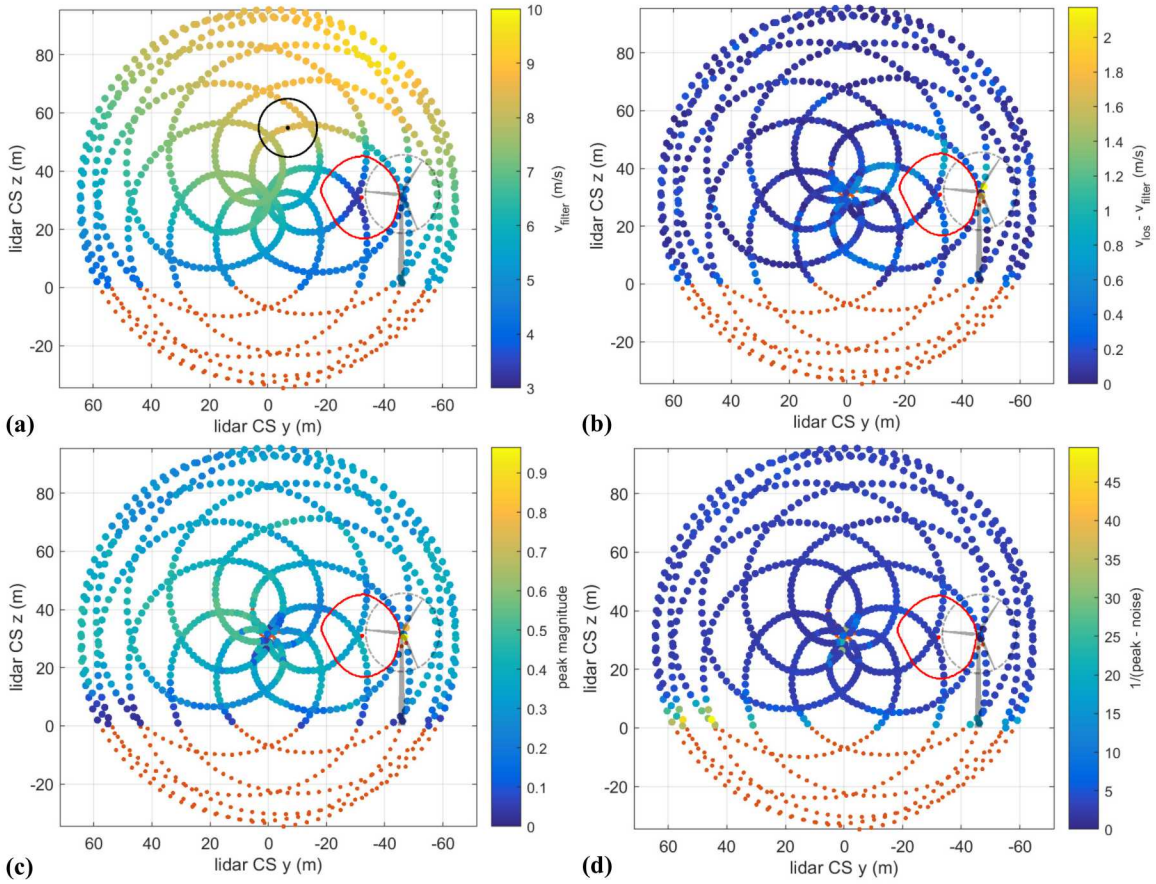

Figure 9. Additional filtering techniques: (a) time-weighted smoothed velocity signal with neighborhood size, (b) velocity difference signal, (c) normalized PDF peak value from returned Doppler spectra, and (d) quality metric of difference between normalized peak value and normalized noise floor.

Finally, Doppler spectra distributions with a low SNR must be removed to ensure valid measurements. This final filter removes low SNR power spectra distributions and is referred to as the quality metric. This outlier detection uses the reciprocal of difference between the peak value in the filtered Doppler spectra PDF and the median value of the noise peaks removed from the filtered Doppler spectra distribution. The noise region is the dark blue region in figure 7. The quality metric was defined as the reciprocal of the difference between the peak and noise (figure 9d). Any value above 20 was

removed. The quality metric threshold corresponds to a peak difference of less than 5% of the maximum possible difference. The 5% value was determined empirically but held well for all focus distances, removing points obscured by ground returns and periods of reduced aerosol within the atmospheric boundary layer.

Figure 10 presents the final quality processed Doppler spectra and scan pattern. The QA/QC process filtered out each of the invalid measurement examples, shown previously in figure 3 leaving only the regions of interest in the velocity field Doppler spectra normalized PDF's of the free stream, wake center, and wake edge cases (figure 10c). The line-of-sight velocity was calculated from the median value of frequencies remaining in the Doppler spectra of figure 10a to produce the v_{los} values in the scan pattern of figure 10b. Figure 10c shows that a highly three-dimensional flowfield, such as the shear layer of the wake edge, can produce a wide distribution of line-of-sight velocities within the probe volume. These distributions of velocities are physically present and important to include in the calculation of the probe volume median v_{los} and higher order line-of-sight velocity statistics, such as turbulence estimation.

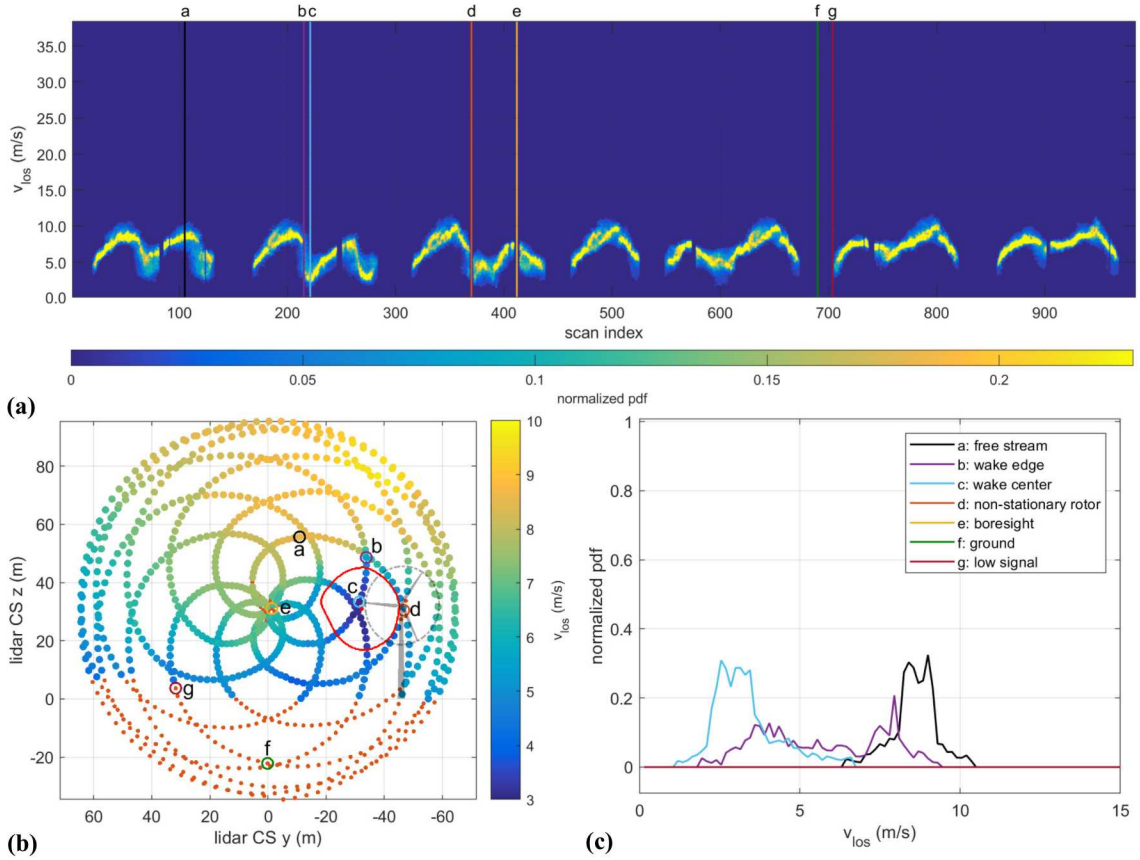

Figure 10. Final Doppler spectra (a) image with lines indicating the example Doppler distributions, (b) scan pattern with wake (red line and center dot), downstream turbine outlined, and example cases marked with circles, and (c) example normalized PDF's of Doppler power spectra traces.

Since the Doppler spectral distributions were concentrated to the regions of interest in the velocity field (figures 10a and 10c), the turbulence of the line-of-sight velocities (v'_{los}) within the probe volume can be estimated more accurately [20]. The reduction in the shot noise in the Doppler spectra using the bilateral filter allows the turbulence to be estimated from the normalized second moment (standard deviation) of the Doppler spectra PDF. The turbulence estimated from the unprocessed Doppler spectra in figure 3 have large errors due to the regions of high signal noise, as shown in figure 11a. The standard deviation of the line-of-sight velocity PDFs within the probe volume is more sensitive to noise than the

median line-of-sight value in figure 3b since it is a higher order statistic. Figure 11b displays the final turbulence field of the example SpinnerLidar scan after the full QA/QC process. The final turbulence field reveals increased turbulence in the shear layer of the wake as one would expect, which is difficult to observe in the unprocessed turbulence field with erroneous values. This finding also corresponds to the distribution of velocities observed within the wake edge example trace in figure 10c. The SpinnerLidar data released on DAP do not yet include the turbulence values, as more work is required to ensure their validity. (e.g. validation against turbulence measurements with conventional anemometry). However, the improved extraction of these quantities helps show the value of implementing such extensive QA/QC methods.

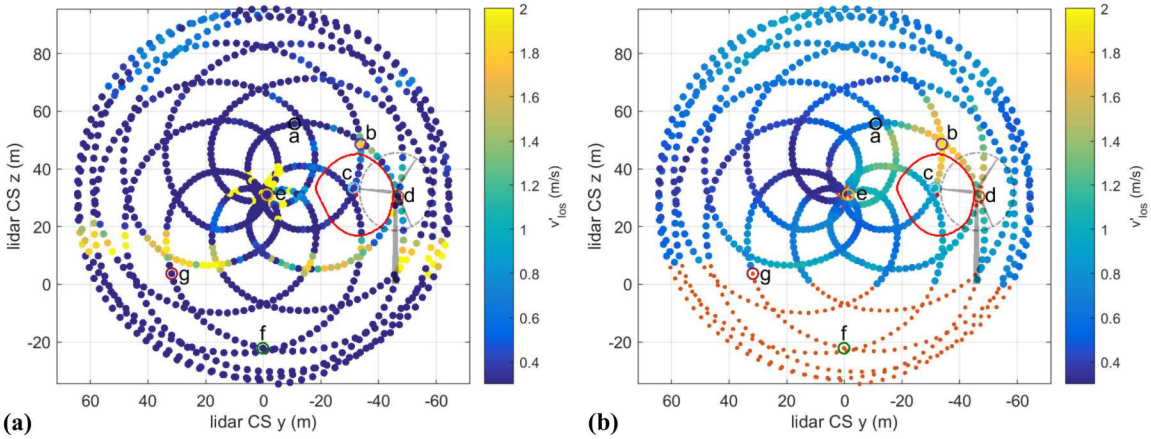

Figure 11. Turbulence estimates (v'_{los}) from the standard deviation of Doppler spectra PDFs: (a) unprocessed data and (b) fully QA/QC'd data scan patterns with wind turbine wake and downstream turbine indicated.

4. Conclusions

The present work details the QA/QC methodology and process developed to ensure the quality of the DTU SpinnerLidar data released on the A2e DAP by filtering out invalid measurements and maximizing data availability within the two-dimensional lidar scans. A multi-dimensional approach to processing the SpinnerLidar Doppler spectra was developed based on matching erroneous measurements within the two-dimensional lidar scan with patterns inside the multidimensional lidar Doppler spectra. This approach allows image processing techniques to be used to remove regions of the Doppler spectra that are contaminated by hard targets and isolate the velocity field. A bilateral filter was used to reduce the noise in the Doppler spectra normalized PDF's and the regions of interest in the velocity field were isolated to improve the accuracy of the line-of-sight velocity measurements and enable the estimation of the turbulence of the line-of-sight velocity within the lidar probe volume. Finally, invalid measurements from an operational rotor and low-signal returns were removed using a 2D sliding neighborhood filter with time weighting and the difference between the peak value and noise floor of each spectral trace, respectively. This work helps ensure and communicate the credibility of the A2e DAP data for future wake model validation efforts and provides new ideas and methodologies for lidar processing and QA/QC approaches.

5. References

[1] Herges T G, Maniaci D C, Naughton B T, Mikkelsen T and Sjöholm M 2017 High resolution wind turbine wake measurements with a scanning lidar *Journal of Physics: Conference Series* **854**

[2] Moriarty P, Rodrigo J S, Gancarski P, Churchfield M, Naughton J W, Hansen K S, Machefaux E, Maguire E, Castellani F, Terzi L, Breton S-P and Ueda Y 2014 IEA-Task 31 WAKEBENCH:

Towards a protocol for wind farm flow model evaluation. Part 2: Wind farm wake models *Journal of Physics: Conference Series* **524** 012185
[3] Hills R G, Maniaci D C and Naughton J W 2015 V&V Framework. In: *SAND-2015-7455,* Sandia National Laboratories
[4] Kelley C L and Ennis B L 2016 SWiFT Site Atmospheric Characterization. In: *SAND-2016-2016*: Sandia National Laboratories
[5] Herges T G, Berg J C, Bryant J T, White J R, Paquette J A and Naughton B T 2018 Detailed analysis of a waked turbine using a high-resolution scanning lidar *Journal of Physics: Conference Series* **1037** 072009
[6] Machefaux E, Larsen G C, Troldborg N, Hansen K S, Angelou N, Mikkelsen T and Mann J 2016 Investigation of wake interaction using full-scale lidar measurements and large eddy simulation *Wind Energy* **19** 1535-51
[7] Churchfield M, Wang Q, Scholbrock A, Herges T, Mikkelsen T and Sjöholm M 2016 Using High-Fidelity Computational Fluid Dynamics to Help Design a Wind Turbine Wake Measurement Experiment *Journal of Physics: Conference Series* **753** 032009
[8] Naughton B 2017 Wake Steering Experiment A2e Data Archive Portal. https://a2e.energy.gov/projects/wake
[9] Clifton A 2014 135-m Meteorological Masts at the National Wind Technology Center: Instrumentation, Data Acquisition and Processing. In: *Technical Report*: National Renewable Energy Laboratory
[10] Frehlich R 1997 Effects of Wind Turbulence on Coherent Doppler Lidar Performance *Journal of Atmospheric and Oceanic Technology* **14** 54-75
[11] Newsom R K, Berg L K, Shaw W J and Fischer M L 2015 Turbine-scale wind field measurements using dual-Doppler lidar *Wind Energy* **18** 219-35
[12] Beck H and Kühn M 2017 Dynamic Data Filtering of Long-Range Doppler LiDAR Wind Speed Measurements *Remote Sensing* **9**
[13] Forsting A R M and Troldborg N 2016 A finite difference approach to despiking in-stationary velocity data - tested on a triple-lidar *Journal of Physics: Conference Series* **753** 072017
[14] Berg J, Bryant J, LeBlanc B, Maniaci D C, Naughton B, Paquette J A, Resor B R, White J and Kroeker D 2014 Scaled Wind Farm Technology Facility Overview. In: *AIAA SciTech 32nd Wind Energy Symposium,*
[15] Sjöholm M, Pedersen A T, Angelou N, Abari F F, Mikkelsen T K, Harris M, Slinger C and Kapp S 2013 Full two-dimensional rotor plane inflow measurements by a spinner-integrated wind lidar. In: *European Wind Energy Association Conference,*
[16] Angelou N and Sjöholm M 2015 UniTTe WP3/MC1: Measuring the inflow towards a Nordtank 500kW turbine using three short-range WindScanners and one SpinnerLidar. DTU Wind Energy
[17] Herges T G, Maniaci D C, Naughton B, Hansen K, Sjöholm M, Angelou N and Mikkelsen T 2017 Scanning Lidar Spatial Calibration and Alignment Method for Wind Turbine Wake Characterization. In: *AIAA SciTech 35th Wind Energy Symposium,*
[18] Peña A, Hasager C B, Lange J, Anger J, Badger M, Bingöl F, Bischoff O, Cariou J-P, Dunne F, Emeis S, Harris M, Hofsäss M, Karagali I, Laks J, Larsen S E, Mann J, Mikkelsen T, Pao L Y, Pitter M, Rettenmeier A, Sathe A, Scanzani F, Schlipf D, Simley E, Slinger C, Wagner R and Würth I 2013 Remote Sensing for Wind Energy. DTU Wind Energy
[19] Phelippeau H, Talbot H, Akil M and Bara S 2008 Shot noise adaptive bilateral filter. In: *2008 9th International Conference on Signal Processing,* pp 864-7
[20] Branlard E, Pedersen A T, Mann J, Angelou N, Fischer A, Mikkelsen T, Harris M, Slinger C and Montes B F 2013 Retrieving wind statistics from average spectrum of continuous-wave lidar *Atmos. Meas. Tech.* **6** 1673-83

Acknowledgments
This work was supported by the U.S. Department of Energy under Contract No. DE-AC04-94AL85000 with Sandia National Laboratories, a multimission laboratory managed and operated by National

Technology and Engineering Solutions of Sandia, LLC, a wholly owned subsidiary of Honeywell International, Inc., for the U.S. Department of Energy's National Nuclear Security Administration under contract DE-NA-0003525. Funding for the work was provided by the Wind Energy Technologies Office within the United States Department of Energy through the Atmosphere to Electrons (A2e) Program. The authors would like to thank the SWiFT support staff, Jonathon Berg, Joshua Bryant, David Mitchell, Miguel Hernandez, and David Martinez. The authors would also like to thank Torben Mikkelsen and Mikael Sjöholm from DTU Wind Energy for their help and expertise installing and using the DTU SpinnerLidar at the SWiFT site in addition to help with data processing discussions. The authors thank Andrew Scholbrock and Donald Baker from the NREL for their support installing the SpinnerLidar at SWiFT. The authors would like to acknowledge Jonathon Berg, Joshua Bryant, Andrew Scholbrock, David Jager, and Jeroen van Dam for their help with supporting and operating the SWiFT wind turbines, and the NREL colleagues working on the Wake Steering Experiment.